

COMBUSTION CHARACTERISTICS BY REVERSED AIR INJECTION AS A FLAMELESS COMBUSTION

Chonggun Choi, Woojin Kim and Donghoon Shin*

*Author for correspondence

Department of Mechanical Engineering,
Kookmin University,
Seoul, 02707,
South Korea,

E-mail: d.shin@kookmin.ac.kr

ABSTRACT

The effort to reduce pollution emission from industrial combustors have been researched through combustion control such as multi staging and flue gas recirculation. Recently, flameless combustion, which is referred as various words such as MILD combustion, HiTAC, etc., has been developed to reduce NO_x and CO simultaneously and to increase heat transfer performance. Meanwhile, those technologies need new concept burner including heat recycling media to heat up combustion air which makes the burner system complicated and expensive. In this research, we introduced a new flameless combustion phenomena generated with reversed air injection technology, which consists of two high speed air nozzles without additional heat recycling media, so it can be operated in a steady mode without alternating flow direction. Experimental study was carried out to investigate the phenomena of reversed air injection. LPG was applied as the fuel. The premixed combustion with metal fiber mat is the relative partner for comparison. As the conclusion, the NO_x emission of the reversed air injection is less than one third of NO_x emission of the premixed combustion. The operation range of heat load increases at the reversed air injection. The CO emission of the reversed air injection at the exit does not increase comparing to the premixed combustion. Aspect ratio of the furnace chamber appears as a main design parameter.

INTRODUCTION

The efforts to reduce pollutants, such as NO_x and CO, generated during the combustion process have been strengthened according to the increased importance of environment [1]. The combustion control methods have been studied for the reduction of NO_x and CO by the exhaust gas recirculation, multi-stage combustion, gas preheating and dilution combustion, etc. [2-5]. The conventional methods have been effective for reducing NO_x and CO individually, however, these methods have difficulty to reduce two pollutants simultaneously.

Flameless combustion named by Wunning[6] is the result of the studies on simultaneous reduction of NO_x and CO. Depending on the combustion condition, flameless combustion has been named as Flameless Oxidation (FLOX) [6-8], High Temperature Air Combustion(HiTAC) [9], Moderate or Intense Low Oxygen Dilution(MILD) [10], Normal Temperature Air Flameless Combustion(NTAFC) [11] and High-temperature

Combustion Technology(HiCOT) [10]. In the flameless combustion technology, the combustion reaction is delayed due to the dilution of the air and fuel with the recirculated combustion gas which results in reduced peak temperature and uniform temperature distribution.

Flameless combustion is implemented by maintaining the temperature of the fluid over the auto ignition temperature. Hosseini et al. [12] achieved temperature condition by preheating of fuel and oxidant using a heat exchanger to recover the heat of the waste gas. Danon et al. [13, 14] preserved the input gas temperature by cross operation of thermal storage mode and combustion mode using regenerative burners made of the honeycomb structure. Meanwhile, flameless combustion needs the delay of the combustion reaction. Li et al. [15] achieved combustion delay by increasing the distance between the fuel nozzle and the oxidant nozzle. Noor et al. [16] showed that dilution of fuel and air with the recirculated exhaust gas is effective. Location and configuration of the nozzle are main design variables in the flameless combustion system. Huang et al. [17] have reported that the combustion limit is changed by the position of the nozzle, and the emission is minimized when air and fuel feed at the bottom of the combustion furnace of hexahedral shape furnace. Mancini et al. [18] have analysed path of NO_x emission of flameless combustion through the experiments and numerical analysis to show that the thermal NO_x process is the main path. The efforts to achieve the flameless condition with ambient temperature injection of fuel and air have been reported. Xing et al. [11] have studied to achieve flameless combustion without preheating process. When the flameless combustion condition is achieved using ambient temperature gas, it has the benefits of reduction of costs for the preheating facility and simplification of the operation and configuration of the combustion system.

In this study, a new combustion method named to Reversed Air Injection (RAI) combustion which has the air injected in the opposite direction of fuel and exhaust gas flow is investigated. The gas compositions and the temperature distribution in the furnace are measured, and design parameters including the combustion method, the heat input rate, and the aspect ratio of the cylindrical furnace were investigated to uncover the combustion characteristics of RAI.

EXPERIMENTAL SETUP

Experimental equipment shown in Fig. 1 consists of a furnace, two mass flow controllers, measuring ports for temperature and gas concentration, and data acquisition device. The furnace shown in Fig. 2 has an inner diameter (D) of 100 mm and changeable height (H) to study effect of the aspect ratio (H/D). A metal fibre burner of which diameter (d_f) is 30mm is installed at the furnace bottom to allow the premixed combustion. In the premixed combustion condition, the fuel and air premixed and fed into the burner. In RAI combustion condition, only fuel is injected to the burner and the air is introduced into two nozzles at the top of furnace. The diameter of air nozzles (d_a) is 1.5mm and the height of nozzle (h_a) is equal to the height of the furnace (H). The radial distance of air nozzles from the furnace axis (r_a) is 40mm. The exit diameter (d_e) is 30mm same as the burner diameter (d_f). The furnace wall has an insulation (Nichias, TOMBO-5420 # 700) which has the thermal conductivity of $0.16 \sim 0.21\text{W/m}\cdot\text{K}$ at $800^\circ\text{C} \sim 1000^\circ\text{C}$ and the thickness of 100mm. The fuel is LPG (C_3H_8 : 60%, C_4H_{10} : 40%), and the oxidant is dry compressor air. Flow rates of the fuel and the oxidant was controlled by the MKP's mass flow controller TSC-230 and TSC-245 respectively. The composition of internal gas and exit gas were measured by SWG-200(MRU) for CO and O_2 in % unit and Testo-330 for CO and NO_x in ppm unit. The temperature was measured by K-type thermo-couple which has wires of 0.6 mm diameter and 0.9 mm bead, and the data were saved to the data acquisition device MV2000(Yokogawa). The ports for internal gas composition and temperature measurement were installed with 100mm intervals along the height of the furnace at the vertical plane including the air jet nozzles. The internal distributions of temperature and gas concentration were measured while the probe moves every 10mm step from the central axis of the furnace to the inner wall at each port. The exhaust gas was measured at the exit port which was installed 200mm above the furnace top. All the measured data at every second were averaged for 3 minutes to be shown at the results.

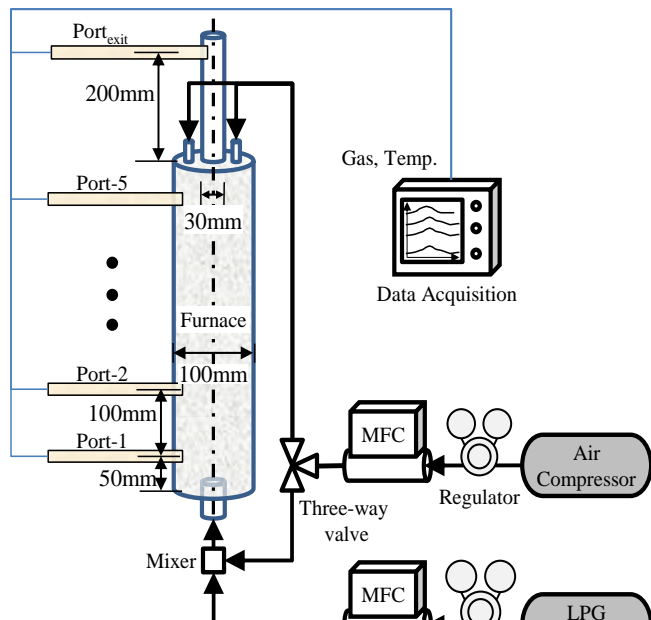


Figure 1 P&ID of experimental setup

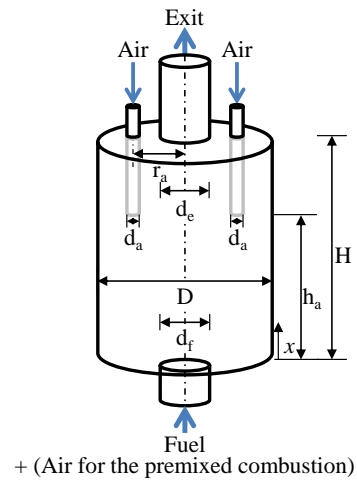


Figure 2 Design parameters of RAI combustor

The heat up of the furnace has been induced in pre-mixed combustion until the average temperature of central axis reaches to 900°C , and then combustion method was shifted to RAI by changing air injection point to the top of the furnace.

The experiments were conducted on three groups as shown in Table 1. The reference operation condition is set to excess air ratio of 10% and ambient pressure. The minimum heat input is 1.89kW when the LPG flow rate is 1.1lpm.

- ① Group A (Case 1,2) : Experiment on combustion mode (pre-mixed combustion and RAI combustion).
- ② Group B (Case 1~8): Experiment on the heat input rate (from 1.89kW to 3.78kW of both combustion modes at $H/D=5$).
- ③ Group C (Case 1,9,10): Experiment on the aspect ratio (H/D : 3,4,5) of RAI combustion. The aspect ratio was set by changing the furnace height from 300 to 500mm.
- ④ Group D (Case 10~13): Experiment on the heat input rate (up to 3.75kW of RAI combustion at $H/D=3$).

Table 1 Experimental conditions

Case No.	Combustion methods	Q_{in}	H/D	$Q_{in}/Vol.$	Air Jet Velocity
		[kW]	[-]	[kW/m ³]	[m/s]
1	Premixed	1.89	5	481	-
2	RAI			642	141
3		2.52		802	
4	Premixed	3.15		963	
5		3.78	5	642	189
6		2.52		802	236
7	RAI	3.15		963	283
8		3.78		602	141
9	RAI	1.89	4	802	
10		2.52	3	1070	189
11		3.15		1337	236
12	RAI	3.15	3	1604	283
13		3.75			

RESULTS AND DISCUSSION

Table 2 shows the overall measurement results of NO_x and CO at the exit port and the average temperature at the centre line.

Table 2 Experimental results

Case No.	NO _x at exit	CO at exit	T1	T2	T3	T4	T5	Stdev.(T)
	[ppm]	[ppm]	°C	°C	°C	°C	°C	°C
1	127	0	1173	1131	1115	1068	1040	47
2	30	0	1062	1120	1192	1171	1131	45
3	133	0	1202	1206	1158	1111	1073	52
4	158	0	1288	1312	1266	1224	1193	43
5	Unstable and lifted flame							
6	41	0	1083	1174	1268	1252	1211	66
7	46	0	1194	1305	1295	1285	1233	42
8	56	0	1225	1334	1322	1302	1262	40
9	25	0	1064	1124	1129	1099	–	26
10	27	0	1186	1189	1153	–	–	16
11	36	0	1208	1207	1177	–	–	14
12	48	0	1257	1264	1231	–	–	14
13	59	0	1306	1313	1275	–	–	17

Group A: Combustion mode

In the premixed condition, CO was not detected and NO_x was 127ppm at the exit port. In RAI combustion with the same operation flow rates, CO also was not detected however NO_x was decreased down to 30ppm. RAI shows the reduction of NO_x emission lower than the premixed condition. Fig. 3 shows the measurement results of the gas concentration and temperature distribution at the cross section of the air nozzle position, which explains the difference of two combustion methods. As shown in Fig. 3(a), the peak temperature of the premixed condition was occurred near the bottom (near the burner), and then it was

cooled down gradually while gas flows toward the exit. In RAI condition, the high temperature appeared near the middle of the furnace, and the temperature distribution was relatively even. The measured peak temperatures were 1173°C in the premixed condition and 1192°C in RAI. Although the measured peak in RAI was higher than the premixed condition, the real peak temperature of the premixed case was expected higher than the measured data because the flame is located at the burner surface below the port1. The O₂ concentration in the premixed combustion showed low concentration near the bottom and then it was maintained a relatively uniform in the upper region as shown in Fig. 3(b). In the RAI combustion, peak O₂ was detected in the middle region in accordance with the trajectory of the air jet. This happened due to lack of penetration of the air jet. Hence the study on the aspect ratio (H/D) of the furnace was conducted subsequently. As shown in Fig. 3 (c), CO of the premixed combustion was not detected at the whole region. CO of RAI mode generated at the bottom region was extinguished by the complete combustion after the middle height. These results show that the combustion reaction of RAI condition occurs at the wide area of upper furnace zone governed by the air jets. As shown in Fig. 3(d), NO_x of the pre-mixed condition intensively generated at the bottom and maintained until the exit. Meanwhile, NO_x of the RAI condition was distributed uniformly in the wide area at low concentration under 50 ppm.

Group B: Heat input

The conditions of the heat input were 1.89(reference case), 2.52, 3.15 and 3.78kW. As shown in Fig. 4, the temperature of the premixed condition has the peak at the bottom and then decreased gradually as the flue gas goes up. The temperature range becomes higher as the heat input increased, which is the main reason of higher NO_x emission. When the heat input is 3.87kW (case 5), the flame of the premixed mode was lifted and unstable, so the measurement data was absent. As the heat input increases, the temperature range increases alike the premixed mode at RAI condition. The position of peak temperature was at

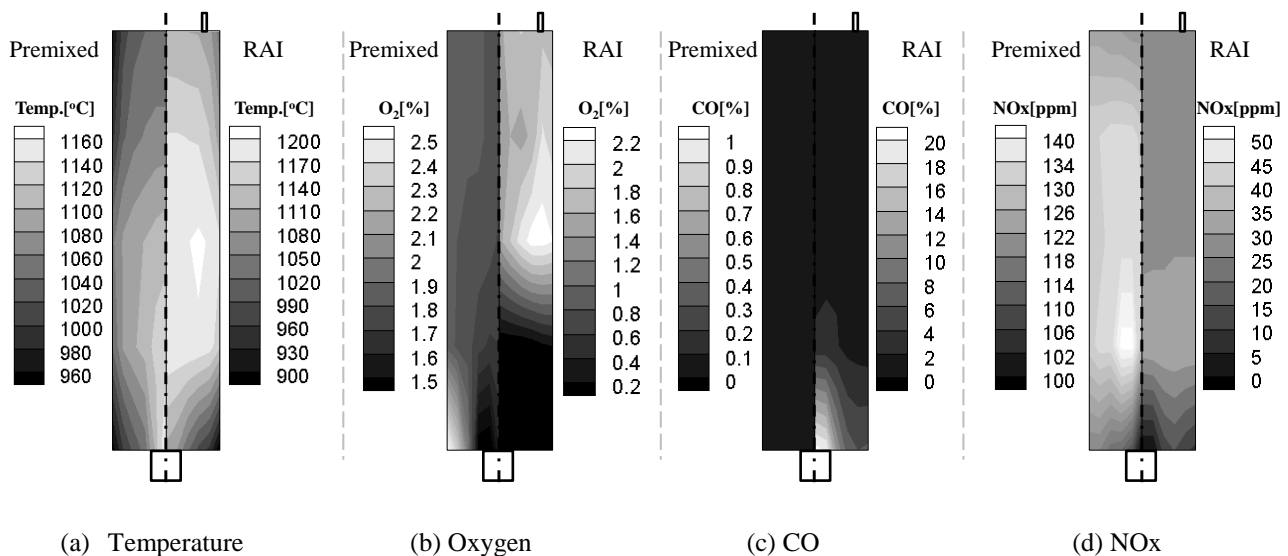


Figure 3 Contours of premixed combustion and RAI combustion with H/D:5 (Case 1,2)

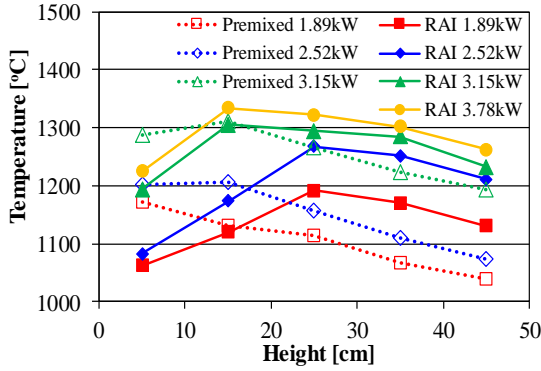


Figure 4 Centreline temperature distributions according to heat input (H/D=5)

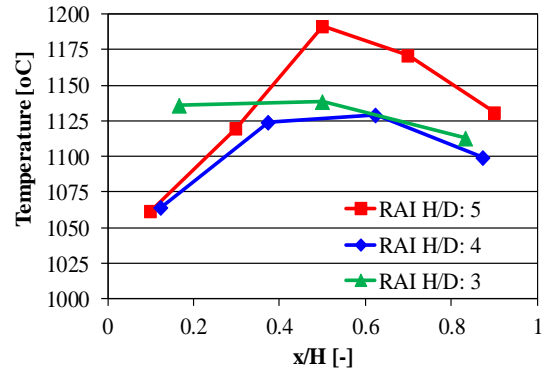


Figure 6 Centreline temperature distributions according to H/D of RAI mode

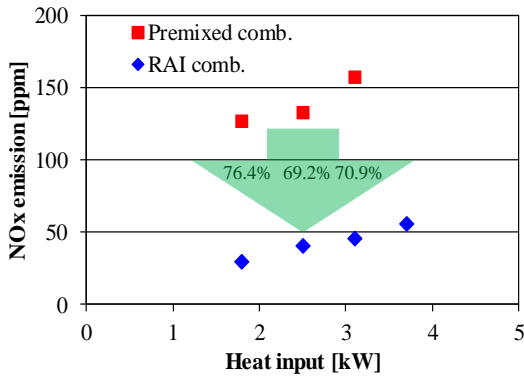


Figure 5 NOx emission depending on heat input at exit port (H/D=5)

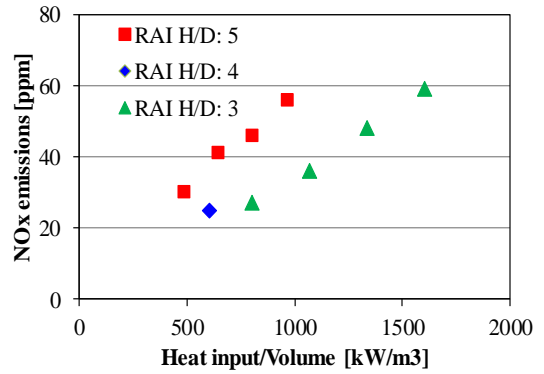
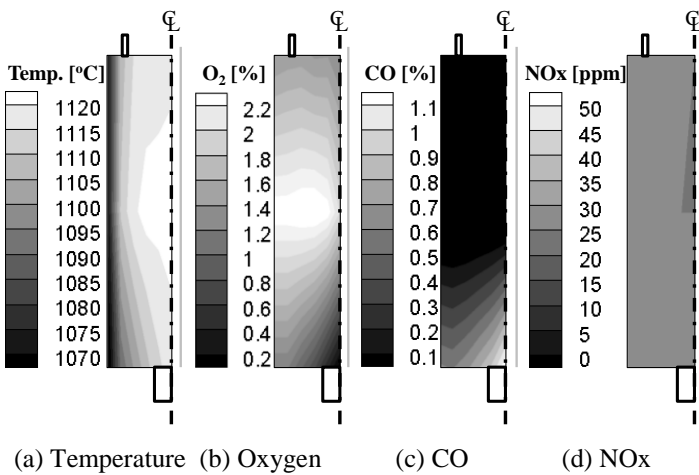


Figure 7 NOx emission depending on heat input per unit volume of RAI mode

the middle (port 3) at 1.89kW and 2.52kW (case 2 and 6). The peak temperature zone moves to the bottom (port 2) in the case of 3.15kW and 3.78kW (case 7 and 8). It is caused by increased reaction due to increased penetration of air jet when reached to the bottom area according to the increased air jet velocity. NOx emission slightly increases according to the increment of heat input, however, the level is one third of the premixed condition in average as shown in Fig. 5.

Group C and D: Aspect ratio (H/D) and heat input of RAI

Experiments on the aspect ratio of 5, 4, and 3 were conducted as changing the furnace height in RAI mode. Fig. 6 shows temperature distribution at the centre line according to the relative height in the furnace. The peak temperature of H/D=5 appears at the middle height and has a difference of 60°C and 130°C to the top and the bottom, respectively. The temperature uniformity increases when H/D decreases which is due to increased reaction uniformity in the furnace volume. NOx emission of H/D=5 as shown in Fig. 7 increases linearly according to the heat input rate. Meanwhile, NOx of H/D=4 and 3 are slightly decreased to 25ppm and 27ppm, although the heat input per unit volume increased to 600kW/m³ and 800kW/m³ respectively. This shows that H/D is an important design parameter to control NOx at elevated heat input for RAI combustion. Fig. 8 shows the measurement results in the furnace of H/D=3. As shown in Fig. 8(a), the trend of temperature distribution was similar to H/D=5. However, the standard deviation at the centre line decreases to 16 °C, which shows that temperature distribution becomes more uniform. The distribution of O₂ concentration also becomes more uniform than H/D=5 (Fig. 8(b)). This result is due to that the air jet reaches to the bottom and the whole area of the furnace is used for the reaction. CO concentration near the bottom of H/D=3 decreased to under 1% (in contrast to H/D=5 with higher than 20%) (Fig.



(a) Temperature (b) Oxygen (c) CO (d) NOx
Figure 8 Contours of RAI combustion with H/D=3 (Case 10)

8(c)). NO_x distribution of H/D=3 is also very even in the total volume (Fig. 8(d)), which correspond to the uniform reaction with the appropriate air jet penetration of RAI mode.

CONCLUSION

This experimental study has performed to find basic characteristics of reversed air injection (RAI) combustion, which feeds the air jet in the reverse direction of the exhaust gas flow without preheating. Premixed combustion using metal fibre mat burner at the cases of 1 and 3-5 is compared to show the different combustion mechanism called flameless combustion of RAI.

Temperature and gas composition in the furnace and at the exit are measured to show uniform reaction over the whole volume at the RAI combustion which is the typical phenomena as the flameless combustion. **The NO_x emission is mainly controlled by the Zeldovich mechanism which has close relation with temperature.** The uniform distribution of temperature **which is lower than the premixed flame temperature,** and **uniform** gas composition of the RAI mode results in **lower** NO_x emission **then the premixed combustion** even at the elevated heat input where the premixed mode cannot achieve **due to flame instability at high velocity.** So the extension of combustion ability of the RAI mode is expected while comparing to the conventional combustion method.

Meanwhile, the aspect ratio of the furnace appeared to be an important design parameter to control the RAI combustion and H/D=3 among 3, 4, and 5 showed the best condition until now.

ACKNOWLEDGEMENT

This work is supported by the Technology Innovation Program (No. 10044583) and the Korea Institute of Energy Technology Evaluation and Planning (KETEP) (No. 20153010031950) funded by the Ministry of Trade, Industry & Energy (MOTIE) of the Republic of Korea.

REFERENCES

- [1] Marilena K. and Elias C., Human health effects of air pollution, *Environmental Pollution*, Vol. 151, 2008, pp. 362-367.
- [2] Zabetta, E. C., Hupa, M. and Saviharju, K. Reducing NO_x Emissions Using Fuel Staging, Air Staging, and Selective Noncatalytic Reduction in Synergy, *Ind. Eng. Chem. Res.*, Vol. 44, 2005, pp. 4552-4561.
- [3] Shim, S. T., Hong, C. H., Kim, B. S., Park, C. S. and Park, K., Effects of Geometrical Variation on Performance of OFA-type Boiler, *Korean Journal of Air-Conditioning and Refrigeration Engineering Conference*, 2012, pp. 854-858.
- [4] Kang, K., Oh, J., Yang, J., Yang, W. and Ryu, C., Biomass co-firing with fuel staging for NO_x emission reduction in coal-fired boiler, *The Korean Society of Combustion Symposium*, 2015, pp. 123-126.
- [5] Han, J. W. and Lee, C. E., Effect of Exhaust Gas Recirculation on CO and NO Emission of Oxygen Enhanced Flame, *The Korean Society of Mechanical Engineers Symposium*, 2002, pp. 1524-1529.
- [6] Wunning, J. A. and Wunning, J. G., Flameless oxidation to reduce thermal NO-formation, *Progress in Energy and Combustion Science*, Vol. 23, 1997, pp. 81-94.
- [7] Hardesty, D. and Weinberg, F., Burners producing large excess enthalpies, *Combustion Science and Technology*, Vol. 8, 1973, pp. 201-214.
- [8] Gupta, A. K., Bolz, S. and Hasegawa, T., Effect of air preheat temperature and oxygen concentration on flame structure and emission, *Journal of Energy Resources Technology - Transactions of the ASME*, Vol. 121, 1999, pp. 209-216.
- [9] Katsuki, M. and Hasegawa, T., The science and technology of combustion in highly preheated air, *Symposium (International) on Combustion*, Vol. 27, 1998, pp. 3135-3146.
- [10] Cavaliere, A. and de Joannon, M., Mild combustion, *Progress in Energy and Combustion Science*, Vol. 30, 2004, pp. 329-366.
- [11] Xing, X., Wang, B. and Lin, Q., Structure of reaction zone of normal temperature air flameless combustion in a 2 ton/h coal-fired boiler furnace, *Proceedings of the Institution of Mechanical Engineers Part A – Journal of Power and Energy*, Vol. 221, 2007, pp. 473-480.
- [12] Hosseini, SE. and Wahid, MA., Biogas utilization: Experimental investigation on biogas flameless combustion in lab-scale furnace, *Energy Conversion and Management*, Vol. 74, 2013, pp. 426-32.
- [13] Danon, B., Cho, E.-S., de Jong, W., and Roekaerts, D.J.E.M., Parametric optimization study of a multi-burner flameless combustion furnace, *Applied Thermal Engineering*, Vol. 31, Issues 14–15, 2011, pp. 3000-3008.
- [14] Cho, E.-S., Danon, B., de Jong, W., and Roekaerts, D.J.E.M., Behavior of a 300 kWth regenerative multi-burner flameless oxidation furnace, *Applied Energy*, Vol. 88, Issue 12, 2011, pp. 4952-4959.
- [15] Li, X., Wei, Z., Xu, L. and Cheng, Y., Effect of inclined angle of fuel jet on NO_x emission in high temperature air combustion, *International Conference on Imaging Systems and Techniques*, 2012, pp. 497–501.
- [16] Noor, M. M., Wandel, Andrew P., and Talal Yusaf., The simulation of biogas combustion in a mild burner, *Journal of Mechanical Engineering and Sciences*, Vol. 6, 2014, pp. 995-1013.
- [17] Huang, M.M., Xiao, Y.H., Zhang, Z.D., Shao, W.W., Xiong, Y., Effect of air/fuel nozzle arrangement on the MILD combustion of syngas, *Applied Thermal Engineering*, Vol. 87, 2015, pp. 200-208.
- [18] Mancini, M., Weber, R. and Bollettini, U., Predicting NO_x emissions of a burner operated in flameless oxidation mode, *Proceedings of the Combustion Institute*, Vol. 29, 2002, pp. 1155-1163.